Multiple-Quantum Coherence Dramatically Enhances the Sensitivity of CH and CH_2 Correlations in Uniformly ^{13}C-Labeled RNA

J. P. Marino,[†] J. L. Diener,[‡] P. B. Moore,[‡] and C. Griesinger*,[†]

Contribution from the Institut für Organische Chemie, Universität Frankfurt, Marie Curie Strasse 11, D-60439 Frankfurt, Germany, and Department of Chemistry, Yale University, 225 Prospect Street, P.O. Box 208107, New Haven, Connecticut 06520-208107

Received December 20, 1996. Revised Manuscript Received April 17, 1997[⊗]

Abstract: One-bond $^1H,^{13}C$ and geminal $^1H,^1H$ dipolar interactions are normally the dominant causes of ^1H and ^{13}C transverse relaxation in NMR experiments applied to $^{13}C,^{15}N$-labeled RNA in solution. Proton,carbon multiple-quantum coherences, where all heteronuclei connected by single bonds are evolved simultaneously in the transverse plane, however, are not affected by these strong dipolar interactions. Consequently, the transverse lifetimes, or T_2 values, of these resonances can be dramatically extended. Here, we show that pulse sequences can be written that take advantage of this effect to enhance the sensitivity with which CH and CH_2 correlations are observed in uniformly $^{13}C,^{15}N$-labeled RNA oligonucleotides. In heteronuclear multiple-quantum correlation experiments, CH and CH_2 correlations are detected with a sensitivity that is enhanced by about a factor of 3 relative to heteronuclear, single-quantum experiments for a $^{13}C,^{15}N$-labeled 36mer RNA oligonucleotide and a constant time period of 25 ms. By including $^1H,^{13}C$ multiple-quantum coherence steps in an $^1H,^{13}C,^{15}N$ NMR experiment of the "out and back" type currently used for through-bond resonance assignment in RNA, we have obtained a sensitivity enhancement of about a factor of 5 in the same 36mer RNA.

Introduction

In solution nuclear magnetic resonance spectroscopy (NMR), the large one-bond heteronuclear $^1H,^{13}C$ and the geminal homonuclear $^1H,^1H$ dipolar interactions are the two chief mechanisms for relaxation of transverse ^{13}C and ^1H magnetization in ^{13}C-labeled macromolecules. However, in the slow tumbling limit characteristic of macromolecules, these principal mechanisms of relaxation are effectively "switched off" for multiple-quantum coherences involving the dipolar-coupled nuclei.[1] Consequently, $^1H,^{13}C$ multiple-quantum coherences should relax more slowly than the single-quantum coherences of the individual ^1H and ^{13}C spins. The increased relaxation times of $^1H,^{13}C$ multiple-quantum coherences relative to ^1H and ^{13}C single-quantum coherences has recently been demonstrated by Bax and Grzesiek[2,3] for uniformly ^{13}C-labeled calmodulin. In that system, methine resonances were detected in a spin-locked constant time heteronuclear multiple-quantum correlation (CT-HMQC) experiment with much better signal-to-noise than the corresponding correlations in a constant time heteronuclear single-quantum (CT-HSQC) experiment.[3]

Here, we use a similar strategy of multiple-quantum line-narrowing to increase the sensitivity with which CH and CH_2 correlations are detected in the spectra of uniformly $^{13}C,^{15}N$-labeled ribonucleic acid (RNA) oligonucleotides. The strategy calls for the generation of $^1H,^{13}C$ zero- and double-quantum coherences for CH groups and triple-spin $^1H,^1H,^{13}C$ single- and triple-quantum coherences for CH_2 groups. Using a 36 nucleotide RNA hairpin, we demonstrate sensitivity enhancements of up to a factor of 3 for $^1H,^{13}C$ heteronuclear correlations for H1′,C1′; H2′,C2′; H3′,C3′; and H4′,C4′ methine groups and for H5′,H5″,C5′ methylene groups. These sensitivity enhancements were evaluated by comparing spectra obtained with 25 ms, multiple-quantum, constant time ^{13}C chemical shift evolution periods and spectra obtained with a conventional 25 ms, single-quantum, constant time evolution periods. We also demonstrate that the incorporation of $^1H,^{13}C$ multiple-quantum coherence steps into the "out and back" type triple-resonance NMR experiments currently used for through-bond assignment of RNAs, such as the $^1H,^{13}C,^{15}N$ (HCN)[4,5] correlation experiment, results in a sensitivity enhancement of about a factor of 5.

NMR Experiments and Simulations

Two pulse sequences have been employed to demonstrate the sensitivity enhancement achieved by using multiple-quantum coherences rather than single-quantum coherences to correlate $^1H,^{13}C$ resonances. Figure 1A shows the CT-HMQC experiment used to correlate ribose H1′,C1′; H2′,C2′; H3′,C3′; and H4′,C4′ resonances, and Figure 1B shows the constant time heteronuclear triple-quantum correlation (CT-HTQC) experiment used to correlate ribose H5′,H5″,C5′ resonances. In these pulse sequences, multiple-quantum coherences of the type $2C_yH_x$ for CH groups (Figure 1A) and $4C_y(H_{1x}H_{2y} + H_{2x}H_{1y})$ for CH_2 groups (Figure 1B) are created before the evolution of ^{13}C chemical shifts during the constant time period, T. Both pulse sequences involve a constant time evolution of ^{13}C chemical shift and are therefore analogous to a conventional constant time heteronuclear single-quantum correlation (CT-HSQC) experiment.[6−8] Since the signal-to-noise ratios observed in these experiments are determined mainly by the relaxation rates of

[†] Universität Frankfurt.
[‡] Yale University.
[⊗] Abstract published in *Advance ACS Abstracts,* July 15, 1997.

(1) Griffey, R. H.; Redfield, A. G. *Q. Rev. Biophys.* **1987**, *19*, 51−82.
(2) Grzesiek, S.; Kuboniwa, H.; Hinck, A. P.; Bax, A. *J. Am. Chem. Soc.* **1995**, *117*, 5312−5315.
(3) Grzesiek, S.; Bax, A. *J. Biomol. NMR* **1995**, *6*, 335−339.
(4) Sklenar, V.; Peterson, R. D.; Rejante, M. R.; Feigon, J. *J. Biomol. NMR* **1993**, *3*, 721−7.
(5) Farmer, B. T., II; Müller, L.; Nikonowicz, E. P.; Pardi, A. *J. Am. Chem. Soc.* **1993**, *115*, 11040−11041.
(6) Santoro, J.; King, G. *J. Magn. Reson.* **1992**, *97*, 202−207.
(7) Vuister, G.; Bax, A. *J. Magn. Reson.* **1992**, *98*, 428−435.

S0002-7863(96)04379-X CCC: $14.00

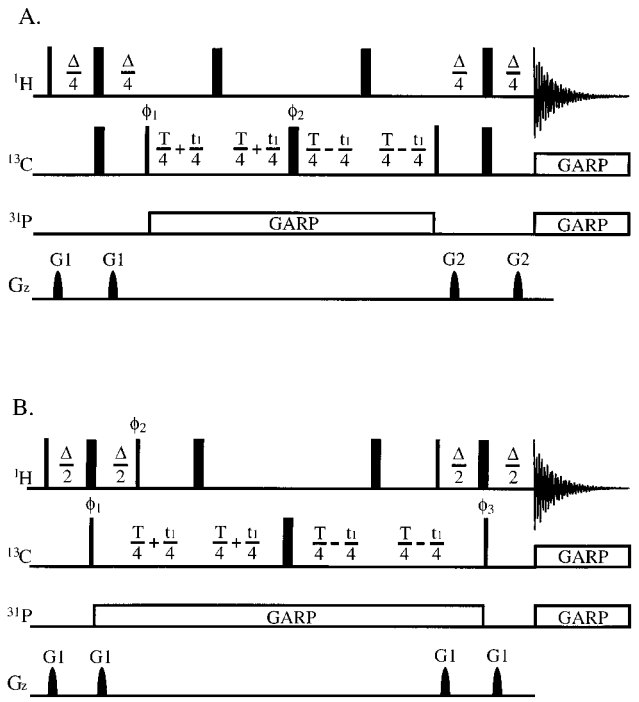

Figure 1. Schematic of the pulse sequence for the CT-HMQC experiment (A) used to correlate CH groups and the CT-HTQC experiment (B) used to correlate CH_2 groups. Narrow and wide vertical lines indicate 90° and 180° flip angle pulses, respectively. All pulses are applied along x unless indicated otherwise. The delays were as follows: $\Delta = 6.0$ ms; $T = 25$ ms. Gradients were applied with a duration of 1 ms and with the strengths $G1 = 2$ G/cm and $G2 = 5$ G/cm for the CT-HMQC experiment (A) and $G1 = 5$ G/cm for the CT-HTQC experiment (B). ^{13}C decoupling was achieved with GARP[18] using a field strength of 2.6 kHz. ^{31}P decoupling was not employed in the experiments. For samples dissolved in H_2O, water suppression can be achieved by combining the pulse sequences in A and B with gradient-enhanced coherence selection schemes, which are based on the generation of heteronuclear gradient echoes.[19] The phase cycle for the CT-HMQC experiment (A) was $\phi_1 = x, -x$; $\phi_2 = 2(x), 2(-x)$; and Rec = $(x, -x)$ and for the CT−HTQC experiment (B) was $\phi_1 = x, -x$; $\phi_2 = 2(x), 2(-x)$; $\phi_3 = 4(x), 4(-x)$; and Rec = $(x, -x, -x, x), (-x, x, x, -x)$. Quadrature detection was obtained in ω_1 by incrementing ϕ_1 in each of the experiments according to States-TPPI.[20]

the spin coherences generated during the CT evolution, comparison of CT-HMQC and CT-HTQC spectra with CT-HSQC spectra can be used to demonstrate the differences in relaxation rates of the different spin coherences.

The CT-HMQC experiment (Figure 1A) used in this study was optimized for the correlation of CH groups in RNA and was derived from a similar experiment originally proposed by Grzesiek and Bax.[3] In the CT-HMQC experiment, heteronuclear double- and zero-quantum coherences $2C_yH_x$ are excited by a 90° proton pulse, followed by a defocusing delay $\Delta/2 = (2J(C,H))^{-1}$, and then a 90° carbon pulse, with proton and carbon 180° pulses applied simultaneously in the middle of this defocusing delay to refocus ^{1}H chemical shifts. The evolution of ^{13}C chemical shifts is then accomplished with refocusing of the ^{1}H chemical shifts, as well as the long-range ^{1}H,^{13}C heteronuclear couplings, using two 180° proton pulses placed in the middle of the $(T - t_1)/2$ and $(T + t_1)/2$ constant time periods. In this experiment, 180° proton pulses are applied during the constant time period, T, in which $2C_yH_x$ coherence evolves instead of a ^{1}H spin-lock as used previously.[3] The spin-lock is omitted because ^{1}H,^{1}H J-dephasing, which results in the 180° proton pulse version of the experiment (Figure 1A), was found to be less detrimental to the signal intensity than the Hartmann−Hahn coherence transfer via ^3J(H,H) couplings, that results in the ^{1}H spin locked version of the experiment. ^{1}H,^{1}H J-dephasing modulates the signal according to the function, $\cos^2(\pi^3 J_{HH}(\Delta + T))$ in the 180° proton pulse version of the experiment, while Hartmann−Hahn coherence transfer modulates the signal according to the function $\cos^2(\pi^3 J_{HH}T)$ $\cos^2(\pi^3 J_{HH}\Delta/2)$ in the ^{1}H spin locked version. In RNA, the severe chemical shift overlap of ribose protons leads to significant Hartmann-Hahn coherence transfer during even a weak continuous wave (CW) spin-lock period.

In Figure 2A, the relaxation decay expected for $2C_yH_x$ multiple-quantum coherences is compared with that predicted for $2C_yH_z$ single-quantum coherence for a H1′,C1′ group in a ribose moiety in an A-form RNA helix. In simulating the effect of dipolar relaxation pathways on the H1′,C1′ group, the dipolar coupling to other proton spins was represented by a pseudospin at a distance of 2.52 Å. In addition, a ^3J(H1′,H2′) coupling of 2 Hz was assumed together with an overall correlation time of 15 ns, which is appropriate for an RNA with a molecular weight of about 12 kDa. It is evident from Figure 2A that the enhancement expected is about a factor of 3 when the constant time delay, T, is set to 25 ms. Figure 2B compares the sum of the 1D traces taken through all H1′,C1′-correlated cross peaks observed in an actual CT-HMQC (bold trace) spectrum with the same sum from a normal CT-HSQC (thin trace) spectrum. Both spectra were obtained from the uniformly ^{13}C-labeled 36mer RNA hairpin used in this study using a constant time delay, T, of 25 ms. The sensitivity enhancement observed is indeed about a factor of 3 and in good agreement with the simulations. Other ^{1}H,^{13}C correlations in this RNA showed similar enhancements with the exception of H3′,C3′-correlated cross peaks which showed an average 2-fold enhancement. The enhancement achieved in these experiments depends on the overall correlation time of the oligonucleotide and, thus, its size. For a 19mer RNA oligonucleotide, we have observed an enhancement of only a factor of 1.5 (data not shown).

To achieve similar enhancement for CH_2 groups, both one-bond ^{1}H,^{13}C heteronuclear and geminal ^{1}H,^{1}H homonuclear dipolar interactions must be "switched off". This is achieved by creating coherences of the type $4C_y(H_{1x}H_{2y} + H_{1x}H_{2y})$, during the evolution of the ^{13}C chemical shift, which do not decay as a result of either geminal ^{1}H,^{1}H or one-bond ^{1}H,^{13}C dipolar coupling within the CH_2 group. The CT-HTQC pulse sequence (Figure 1B) used to achieve this goal excites heteronuclear triple- and single-quantum coherences $4C_y(H_{1x}H_{2y} + H_{1x}H_{2y})$ by first applying a 90° proton pulse, followed by a defocusing delay $\Delta/2 = (2J(C,H))^{-1}$, and then applying a carbon 90° proton pulse to create the double-quantum coherence $2C_y(H_{1x} + H_{2x})$ as in the first experiment. A second defocusing delay, $\Delta/2 = (2J(C,H))^{-1}$, followed by a 90° proton pulse then creates the triple and single-quantum coherences $4C_y(H_{1x}H_{2y} + H_{1x}H_{2y})$. A proton 180° pulse is applied simultaneously with the carbon 90° pulse to refocus ^{1}H chemical shifts during the period Δ. The evolution of ^{13}C chemical shifts is then accomplished with refocusing of the ^{1}H chemical shifts as well as of long-range ^{13}C,^{1}H heteronuclear couplings by two 180° proton pulses in the middle of $(T - t_1)/2$ and $(T + t_1)/2$ constant time periods. The constant time period between the carbon 90° pulses is again set to 25 ms, but in this experiment the t_{1max} is limited to $(T - \Delta) = 19$ ms due to the need to create the triple-quantum coherence during the second defocusing/refocusing delay. As in the CT-HMQC pulse sequence, proton 180° pulses are applied during the constant time period in which $4C_y(H_{1x}H_{2y} + H_{1x}H_{2y})$

(8) van de Ven, F. J. M.; Philippens, M. E. P. *J. Magn. Reson.* **1992**, *97*, 637−644.

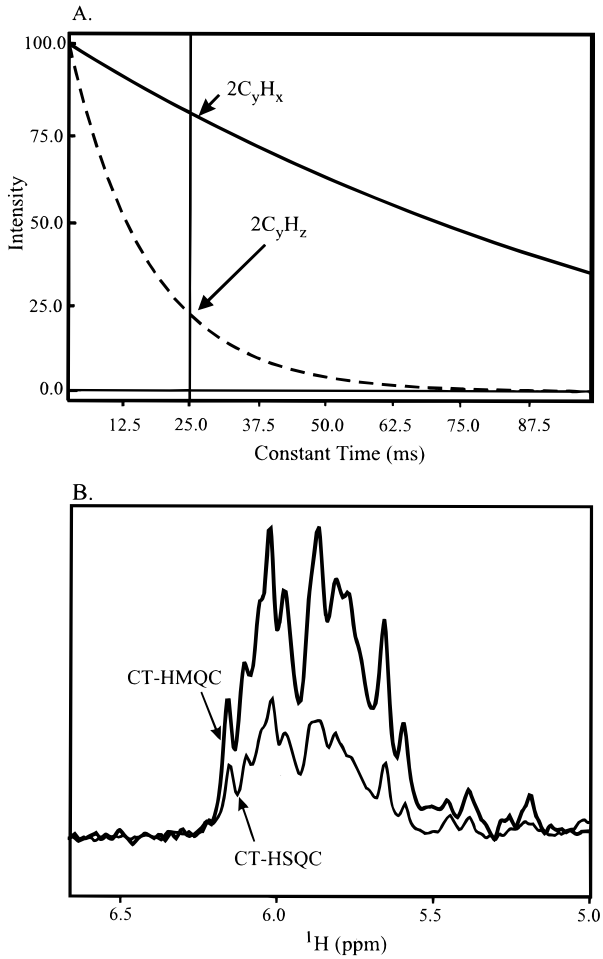

Figure 2. (A) Simulation of the decay of the heteronuclear coherences generated from a two-spin CH system performed using the program wtest.[17] For the CH spin system, the H1′,C1′ was considered with $r_{H1',C1'}$ = 1.1 Å; the ^3J(H1′,H2′) coupling assumed to be ∼2 Hz, the overall correlation time set to 15 ns, and the homonuclear H,H relaxation considered via a pseudospin at a distance of 2.52 Å (this was calculated using distances generated from A-form helical geometry in the program InsightII). The curves showing the decay of the $2C_yH_x$ (solid line) coherence as observed in the CT-HMQC pulse sequence (Figure 1A) and the 2 C_yH_z (dashed line) coherences as observed in a conventional CT-HSQC demonstrate the difference in relaxation behavior. The 25 ms time point is indicated to show the magnitude of the multiple-quantum $2C_yH_x$ (80%) and single-quantum $2C_yH_z$ (23%) magnetization that remains at this point. (B) A comparison of traces showing the 1D summations over the H1′,C1′ correlated regions of the CT-HMQC (bold trace) and a conventional CT-HSQC (thin trace) experiments performed on the uniformly ^{13}C-labeled 36mer RNA oligonucleotide. All experiments were collected with the same spectral parameters and conditions and processed identically using Felix95 on a Silicon Graphics workstation. The details of the experimental and processing parameters are given in the Experimental Section.

coherence evolves rather than a ^{1}H spin-lock in order to avoid Hartmann−Hahn coherence transfer, which would again lead to a general reduction in the signal-to-noise. In addition, any spin-locking sequence with an appreciable duty ratio (DR) would generate the two very fast relaxing coherences $4C_y(H_{1z}H_{2x} + H_{1x}H_{2z})$ during the DR/2 fraction of the spin-lock period and thus reduce the lifetime of the desired coherence (Figure 3A). Therefore, as few 180° proton pulses as possible are recommended. For proton resonance broadening by exchange, short 180° proton pulses (∼20 μs) separated by short delays (500 μs) were successfully employed.

As for H1′,C1′ groups, a series of simulations were done to explore the relaxation behavior of the various spin coherences

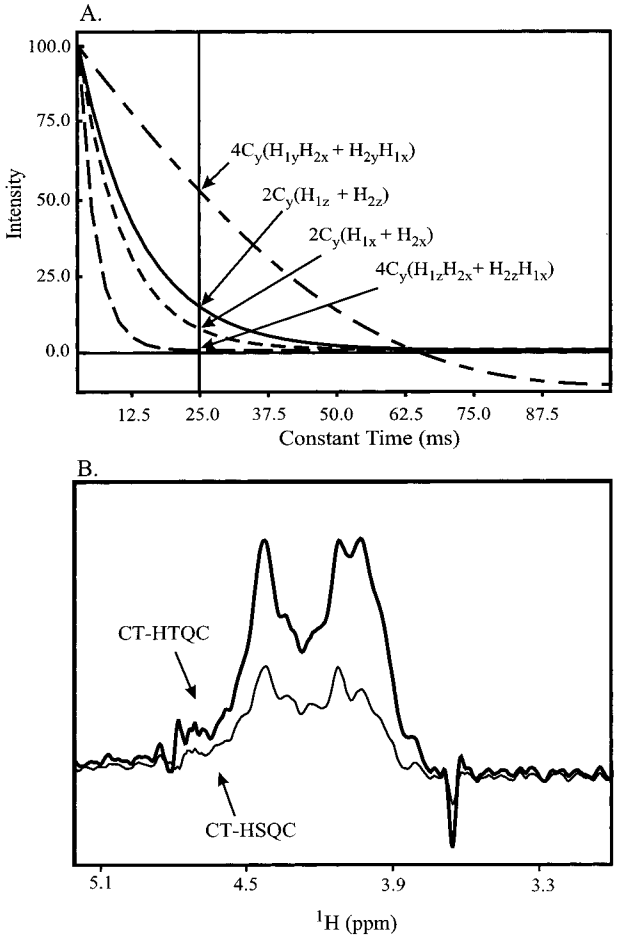

Figure 3. Simulation of the decay of the heteronuclear coherences generated from a three-spin CH_2 system performed using the program wtest.[17] For the CH_2 spin system, the C5′,H5′/H5″ nuclei have been considered with ^2J(H5′,H5″) = −12 Hz, $r_{C5',H5'}$ = 1.1 Å, and $r_{H5',H5''}$ = 1.78 Å and the homonuclear H,H relaxation considered via a pseudo-atom with a distance of 2.52 Å. Both ^3J(H4′,H5′) couplings were assumed to be 4 Hz, and the overall correlation time set to 15ns. Full cross correlated relaxation was taken into account for the CH_2 spin system. The curves showing the decay of the $4C_y(H_{1y}H_{2x} + H_{1x}H_{2y})$ coherence (long−short dashed line) as observed in the CT-HTQC pulse sequence (Figure 1B), the $2C_y(H_{1z} + H_{2z})$ coherences (solid line) as observed in a conventional CT-HSQC, the $2C_y(H_{1x} + H_{2x})$ coherences (short dashed line) as generated by the CT-HMQC, and the $4C_y(H_{1z}H_{2x} + H_{1x}H_{2z})$ coherence (long dashed line) that would be generated by a proton 90$_x$° pulse from $4C_y(H_{1y}H_{2x} + H_{1x}H_{2y})$. For the CH_2 spin system, the $4C_y(H_{1z}H_{2x} + H_{2z}H_{1x})$ coherence decays the fastest (0.1% remains after 25 ms), while about 52% of the $4C_y(H_{1y}H_{2x} + H_{1x}H_{2y})$ coherence remains at a constant time of 25 ms as indicated. The magnetization remaining for the other two coherences after 25 ms was 14% for $2C_y(H_{1z} + H_{2z})$ and 6.0% for $2C_y(H_{1x} + H_{2x})$. (B) A comparison of traces showing the 1D summations over the C5′,H5′/H5″-correlated regions of the CT-HTQC (bold trace) and a conventional CT-HSQC (thin trace) experiments performed on the uniformly ^{13}C-labeled 36mer RNA oligonucleotide. All experiments were collected with the same spectral parameters and conditions and processed identically using Felix95 on a Silicon Graphics workstation. The details of the experimental and processing parameters are given in the Experimental Section.

that can be generated from a H5′,H5″,C5′ spin system (Figure 3A). It is clear from the simulations that the triple- and single-quantum coherences $4C_y(H_{1y}H_{2x} + H_{1x}H_{2y})$ have the longest lifetimes and that the $2C_y(H_{1x} + H_{2x})$ and $4C_y(H_{1z}H_{1x} + H_{1z}H_{2x})$ coherences decay the fastest. This is because the $2C_y(H_{1x} + H_{2x})$ and $2C_y(H_{1z}H_{1x} + H_{1z}H_{2x})$ coherences are very efficiently relaxed through dipolar interaction with the second geminal proton. The $4C_y(H_{1z} + H_{2z})$ coherences observed in a CT-

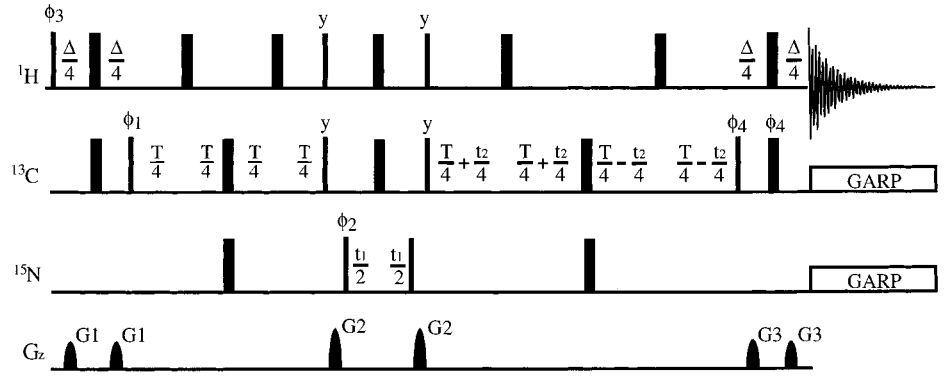

Figure 4. Schematic of the pulse sequences for the 3D MQ-HCN experiment. Narrow and wide vertical lines indicate 90° and 180° flip angle pulses, respectively. All pulses are applied along *x* unless indicated otherwise. The delays were as follows: $\Delta = 6.0$ ms; $T = 25$ ms. Gradients were applied with a duration of 1 ms and with the strengths $G1 = 2$ G/cm, $G2 = 5$ G/cm, and $G3 = 2$ G/cm. ^{13}C decoupling was achieved with GARP[18] using a field strength of 2.6 kHz. ^{15}N decoupling was not employed in the experiment. The phase cycle for the 3D MQ-HCN experiment was $\phi_1 = x, -x$; $\phi_2 = 2(x), 2(-x)$; $\phi_3 = 4(x), 4(-x)$; and Rec = $(x, -x, -x, x), (-x, x, x, -x)$. Quadrature detection is obtained in ω_1 by incrementing ϕ_2 and in ω_2 by incrementing ϕ_4 according to States-TPPI.[20]

HSQC experiment behave in much the same way; however, quantitative analysis reveals that they decay slower than the double- and zero-quantum coherences. For the actual CT-HTQC experiment, the enhancement of a factor of 3.5 as predicted from the relaxation curves is not fully realized since additional defocusing and refocussing delay ($\Delta/2$) periods amounting to 6 ms are required to generate triple-quantum coherences. The rather fast relaxation of spin coherence during these additional delays reduces the enhancement for the CT-HTQC experiment by approximately two-thirds (simulations not shown). In practice, therefore, an enhancement of up to a factor of 2.5 is expected for a CT-HTQC experiment with a constant time of 25 ms applied to a 36mer RNA oligonucleotide. Figure 3B compares the sum of all the 1D traces taken through all H5′,H5″,C5′-correlated cross peaks from the CT-HTQC experiment (bold trace) with the same sum from a CT-HSQC experiment (thin trace). Both experiments were done on the same uniformly ^{13}C-labeled 36mer RNA hairpin with a constant time delay of 25 ms. The average sensitivity enhancement observed is about a factor of 2.5 as expected based on the simulations.

The CT-HMQC and CT-HTQC pulse sequence elements described here can be used to enhance the sensitivity and resolution of ^{13}C-separated 3D and 4D experiments done on RNA. In addition, these pulse sequence elements can be incorporated into the HCX (where X is ^{15}N, ^{13}C, or ^{31}P) "out and back" type heteronuclear-correlated NMR experiments, which are used for the through-bond assignment of ^{13}C,^{15}N-labeled RNAs.[4,5,9−12] Here, we demonstrate their dramatic impact on an HCN correlation experiment.[4,5] In the MQ-HCN (Figure 4), ^{1}H,^{13}C multiple-quantum coherence steps are employed for the two 25 ms periods used to defocus and refocus the long-range ^{13}C,^{15}N heteronuclear couplings. As in the CT-HMQC experiment, heteronuclear double- and zero-quantum coherences $2H_xC_x$ are excited by the first 90° proton pulse followed by a defocusing delay $\Delta/2 = (2J(C,H))^{-1}$ and then a 90° carbon pulse, with proton and carbon 180° pulses applied simultaneously in the middle of this defocusing delay to refocus ^{1}H chemical shifts. In the first half of the experiment, the defocusing of ^{13}C,^{15}N coupling is accomplished with refocusing of the ^{1}H chemical shifts, as well as long-range ^{1}H,^{13}C heteronuclear couplings, by placing proton 180° pulses in the middle of two $T/2$ periods. In order to evolve ^{15}N single-quantum coherences during t_1, proton and carbon $90_y°$ pulses are applied together with a nitrogen $90_x°$ pulse to create $4H_zC_zN_y$ coherences. These coherences are converted back to ^{1}H,^{13}C multiple-quantum coherences antiphase to the nitrogen after the t_1 evolution by again applying proton and carbon $90_y°$ pulses together with a nitrogen $90_x°$ pulse. In the second half of the experiment, the constant time evolution of ^{13}C chemical shifts is accomplished together with refocusing of the ^{13}C,^{15}N coupling, while ^{1}H chemical shifts as well as long-range ^{1}H,^{13}C heteronuclear couplings are again refocused by proton 180° pulses placed in the middle of $(T - t_1)/2$ and $(T + t_1)/2$ constant time periods. Figure 5 shows that the 2D version of the MQ-HCN experiment is about five times more sensitive than a conventional 2D HCN experiment. The full 2D ^{1}H,^{15}N-correlated plots for the MQ-HCN and HCN experiments, which were designed to correlate anomeric H1′ protons with their one-bond C1′ carbons and two-bond-connected base nitrogens (N1/N9), are shown in Figure 5A and 5B, respectively. Both spectra have been acquired and processed identically and are plotted using the same number of contours and levels. Most of the correlations observed in the 2D MQ-HCN experiment (Figure 5A) are lost in the noise in the conventional 2D HCN experiment (Figure 5B). Arrows labeled 1, 2, and 3 indicate the frequency in the ^{15}N dimension at which representative 1D traces were taken from both the HCN and MQ-HCN experiments for comparison. The traces in Figure 5C (HCN shown as the lower thin lines and MQ-HCN as the upper bold lines) clearly show the enhancement achieved for representative uridine H−N1 correlations (1), cytidine H−N1 correlations (2), and purine H−N9 correlations (3).

Discussion

The exploitation of proton,carbon multiple-quantum coherence results in dramatic improvements in the sensitivity of heteronuclear NMR experiments done on RNA oligonucleotides. We have demonstrated that 25 ms CT-HMQC and CT-HTQC pulsed NMR experiments are more sensitive than 25 ms CT-HSQC experiments by a factor of 3 for a 36 nucleotide RNA oligonucleotide. The use of these pulse sequence elements will improve the sensitivity and resolution of ^{13}C-separated 3D and 4D NMR experiments applied to RNA. In ^{13}C-separated experiments, the problem of ^{13}C resonance overlap becomes

(9) Heus, H. A.; Wijmenga, S. S.; van de Ven, F. J. M.; Hilbers, C. W. *J. Am. Chem. Soc.* **1994**, *116*, 4983−4984.
(10) Marino, J. P.; Schwalbe, H.; Anklin, C.; Bermel, W.; Crothers, D. M.; Griesinger, C. *J. Am. Chem. Soc* **1994**, *116*, 6472−6473.
(11) Wijmenga, S. S.; Heus, H. A.; Leeuw, H. A.; Hoppe, H.; van, d. G. M.; Hilbers, C. W. *J. Biomol. NMR* **1995**, *5*, 82−6.
(12) Marino, J. P.; Schwalbe, H.; Anklin, C.; Bermel, W.; Crothers, D. M.; Griesinger, C. *J. Biomol. NMR* **1995**, *5*, 87−92.

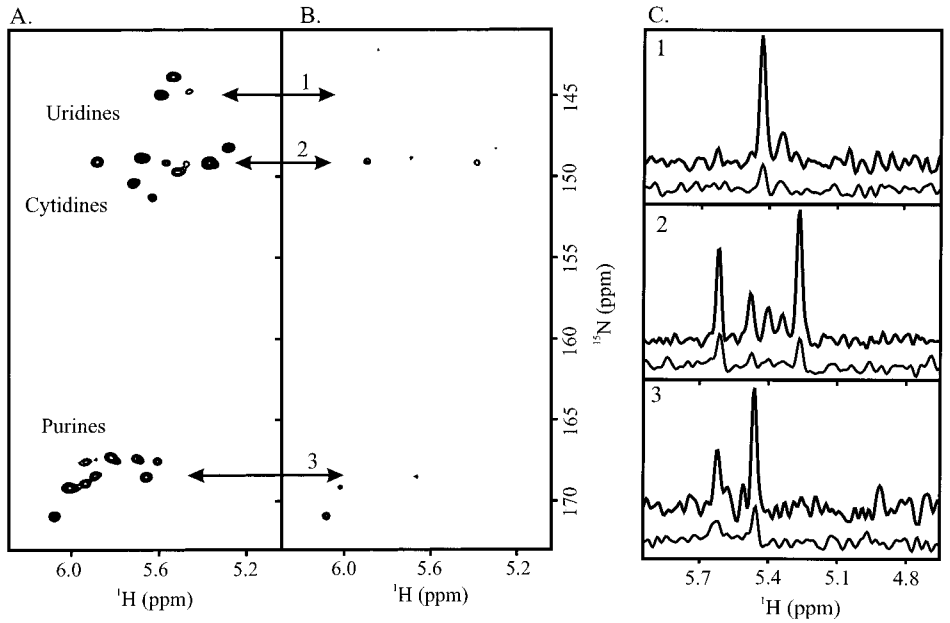

Figure 5. Plot of the ^{1}H,^{15}N correlations observed in a 2D version of the MQ-HCN (A) and the conventional HCN (B) experiments. Both spectra are plotted at the same contour level and with same number of contours. Arrows labeled 1, 2, and 3 indicate the frequency in the ^{15}N dimension at which representative 1D traces through cross peaks have been taken from both the HCN and MQ-HCN experiments for comparison. These traces from the MQ-HCN (bold upper trace) and the HCN (thin lower trace) are shown in panel C for representative uridine H−N1 correlations (1), cytidine H−N1 correlations (2), and purine H−N9 correlations (3).

obviously greater as the size of the RNA increases. Longer ^{13}C chemical shift evolution periods, which are required to improve resolution, increase the impact of homonuclear ^{13}C,^{13}C couplings and lead to a reduction in sensitivity and resolution. The improvement provided by the sensitivity enhanced, multiple-quantum constant time evolution of ^{13}C chemical shifts will therefore be critical for the more complete interpretation of the spectra generated with larger RNAs, especially for the rather poorly dispersed ^{13}C ribose carbon resonances. In addition, as we have shown for the HCN experiment, these ^{1}H,^{13}C multiple-quantum pulse sequence elements can be incorporated with dramatic results into the HCX correlated triple-resonance NMR experiments currently used for through-bond assignment of ^{13}C,^{15}N-labeled RNAs. In these HCX experiments, the ^{1}H,^{13}C multiple-quantum pulse sequence element can be employed in the two 25 ms periods when the long-range heteronuclear couplings are first defocused and then refocused. Using this strategy, we observed an enhancement of up to a factor of 5 for correlations in an MQ-HCN experiment relative to a standard HCN experiment.

In RNA, we find that the sensitivity enhancement realized by the evolution of multiple-quantum coherence rather than single-quantum coherence is significantly greater than that observed for proteins of the same molecular weight and overall correlation times.[2,3] We believe the reason for this observation is that the density of protons is significantly lower in RNA than in proteins. In RNA molecules, therefore, methine and methylene groups behave more like isolated spin systems. For example, the proton pseudospin has been calculated to be on average less than 2.0 Å away for C_α protons in proteins,[3] while in this study it has been calculated to be about 2.52 Å away for H1′ protons in RNA. As a result of this difference in distance, the contribution of the pseudospin to the dipolar relaxation rates of ^{1}H,^{13}C multiple-quantum coherences generated from $C_\alpha H_\alpha$ moieties in proteins is about five times larger than it is for the ^{1}H,^{13}C multiple-quantum coherences generated from H1′,C1′ moieties in RNA. Since the contribution of the pseudospin relaxation is significantly smaller in RNA than in proteins, random deuteration strategies which have proved to be successful in improving the sensitivity of protein spectra will probably have a smaller impact on the sensitivity of RNA spectra.

The use of multiple-quantum pulse sequence elements will not only improve the sensitivity and resolution of ^{13}C experiments applied to RNA but also increases the magnitude of the improvement with the size of RNA molecules under investigation. The effect of "switching off" dipolar relaxation pathways will become more pronounced for slower tumbling macromolecules with longer correlation times. We therefore expect that the use of multiple-quantum coherence correlations will dramatically increase the size of ^{13}C,^{15}N RNA labeled oligonucleotides to which heteronuclear correlated experiments can now be successfully applied.

Experimental Section

A. Sample Preparation. The sequence of the 36mer RNA stem-loop used in this study was 5′-rGGUGACUCCAGAGGUCGAGAGAC-CGGAGAUAUCACC-3′. It was derived from the halophilic archeon *Halobacterium volcanii* $tRNA^{trp}$ intron/exon splicing junction.[13] The RNA oligonucleotide was synthesized by T7 run-off transcription and purified using standard gel electrophoresis methods.[14] The ^{13}C,^{15}N NTPs were prepared from RNA isolated from *Escherichia coli* grown in minimal media with [^{13}C]glucose and $^{15}NH_4Cl$ as the sole carbon and nitrogen sources, respectively.[15,16] The NMR sample was prepared to contain ∼2.0 mM oligonucleotide in 99.96% D_2O, 80 mM NaCl, 0.1 mM EDTA, and 5 mM PO_4^{-2} [pH = 6.7]. The experiments were measured in a Shigemi limited volume NMR tube with a sample volume of ∼170 μL.

B. Acquisition and Processing of NMR Data. The CT-HMQC (Figure 1A), CT-HTQC (Figure 1B), and MQ-HCN (Figure 4), as well as the standard CT-HSQC[6,7] and HCN[4,5] experiments, were all recorded at 288 K on a Varian Unity Plus spectrometer equipped with a triple-resonance ^{1}H,^{13}C,^{15}N probe with actively shielded *z*-gradients and linear amplifiers on all three channels. The CT-HMQC, CT-HTQC, and CT-

(13) Thompson, L.; Danials, C. *J. Biol. Chem.* **1990**, *265*, 18104−18111.
(14) Milligan, J. F.; Uhlenbeck, O. C. *Methods Enzymol.* **1989**, *180*, 51.
(15) Batey, R. T.; Inada, M.; Kujawinski, E.; Puglisi, J. D.; Williamson, J. R. *Nucleic Acids Res.* **1992**, *20*, 4515−23.
(16) Nikonowicz, E. P.; Sirr, A.; Legault, P.; Jucker, F. M.; Baer, L. M.; Pardi, A. *Nucleic Acids Res.* **1992**, *20*, 4507−13.

HSQC were all collected with 512 (t_2^{max} = 93 ms) and 114 (t_1^{max} = 19 ms) complex points in ω_2 and ω_1, respectively. The carbon transmitter frequency was centered on the ribose region of spectrum (∼78 ppm), and the proton transmitter was centered on the residual HDO signal (∼4.75 ppm). For each experiment, 32 scans per t_1 increment were collected with spectral widths of 5500 and 6000 Hz in ω_2 and ω_1, respectively. The total experiment time for each was 4.5 h. The 2D HCN and 2D MQ-HCN (Figure 4) were both collected with 512 (t_2^{max} = 93ms) and 175 (t_1^{max} = 25 ms) complex points in ω_2 and ω_1, respectively. The carbon transmitter frequency was centered on the C1′ region of the spectrum (∼91 ppm), the nitrogen transmitter frequency was centered between the N9 and N1 regions of the spectrum (∼155 ppm), and the proton transmitter was centered on the residual HDO signal (∼4.75 ppm). Forty-eight scans per t_1 increment were collected with spectral widths of 5000 and 5000 Hz in ω_2 and ω_1, respectively. The total experiment time for each was 10 h.

All spectra were processed using Felix95 software (MSI) on a Silicon Graphics workstation. The CT-HMQC, CT-HTQC, and CT-HSQC were processed with sine-bell apodization shifted by 60° applied in both dimensions, and the data were zero-filled to yield a final matrix size of 1024 × 1024 real points. The 2D HCN and 2D MQ-HCN were processed with squared sine-bell apodization shifted by 50° applied in both dimensions, and the data were zero-filled to yield a final matrix size of 1024 × 1024 real points.

Simulation of the decay of various heteronuclear coherences generated from the two-spin CH and three-spin CH_2 systems were performed using the program wtest.[17] Curves were displayed using Felix95 software (MSI) on a Silicon Graphics workstation.

Acknowledgment. This work was supported by grants from the Fonds der Chemischen Industrie and the DFG to C.G. and by a grant from NIH to P.B.M. (GM-41651). J.P.M. acknowledges an Alexander von Humboldt post-doctoral fellowship and thanks D. M. Crothers for support (NIH grant GM-21966) and insightful discussions on the subject.

JA964379U

(17) Madi, Z. L.; Ernst, R. R. Personal communication.

(18) Shaka, A. J.; Barker, P.; Freeman, R. J. *J. Magn. Reson.* **1985**, *64*, 547−552.

(19) Hurd, R. E. *J. Magn. Reson.* **1990**, *87*, 422. Kay, L. E.; Keifer, P.; Saarinen, T. *J. Am. Chem. Soc.* **1992**, *114*, 10663−10664. Schleucher, J.; Sattler, M.; Griesinger, C. *Angew. Chem.* **1993**, *105*, 1518−1521; *Angew. Chem., Int. Ed. Engl.* **1993**, *32*, 1489−1491. Schleucher, J.; Schwendinger, M.; Sattler, M.; Schmidt, P.; Schedletzky, O.; Glaser, S. J.; Sørensen, O. W.; Griesinger, C. *J. Biomol. NMR* **1994**, *4*, 301−306.

(20) Marion, D.; Ikura, R.; Tschudin, R.; Bax, A. *J. Magn. Reson.* **1989**, *85*, 393.